

# Synthesis and electrochemical analysis of $\text{AlVMoO}_7$ oxide prepared via sol–gel method

D SARITHA

Department of Chemistry, K L University, Hyderabad 500075, India  
sarithaitm@gmail.com

MS received 15 May 2017; accepted 2 October 2017; published online 16 May 2018

**Abstract.** In this study,  $\text{AlVMoO}_7$  phase was fruitfully synthesized by sol–gel method and investigated as electrode material. The role of trivalent cation Al on the position of V and Mo redox couples in a three-dimensional framework of  $\text{AlVMoO}_7$  promoted us to use this compound. The electrochemical insertion of Li in this phase was characterized by both solid solution and two-phase regimes. In the voltage range of 3.2–1.5, the first cycle discharge capacity value was found to be 310 mAh  $\text{g}^{-1}$ . It showed very good capacity of 180 mAh  $\text{g}^{-1}$  even after 20 cycles.

**Keywords.** 3D structure;  $\text{AlVMoO}_7$ ; electrochemical Li insertion.

## 1. Introduction

Polyanionic compounds are more favourable as positive electrode materials than the currently used ones, owing to their superior electrochemical features, environmental easiness and low-cost for lithium batteries (layered  $\text{LiCoO}_2$  and spinel  $\text{LiMn}_2\text{O}_4$ ) [1]. Among these compounds, olivine  $\text{LiFePO}_4$ , amorphous  $\text{FePO}_4$  and nasicon  $\text{Li}_3\text{Fe}_2(\text{PO}_4)_3$  were broadly studied [1]. The phosphate  $(\text{PO}_4)^{3-}$  framework present in these compounds acts as the structural stabilizer during the electrochemical reactions. The specific capacity of these electrodes is limited due to the electrochemical inertness of these electrodes compared to the vanadium- and molybdenum-based polyanions [2]. The vanadium- and molybdenum-based polyanions provide numerous metal oxidation states, structural stability as well as a high theoretical specific capacity which could be replaced by phosphate- and sulphate-based polyanion groups. These oxides were recognized as positive electrode materials [2–7]. Based on the advantages associated with them, the present work was focussed on polyanion compound  $\text{AlVMoO}_7$ , which contains both vanadium and molybdenum as electroactive species.

There are several studies on vanadium- and molybdenum-based oxides in the literature. Vanadium containing phases, such as  $\text{VO}_2$  (B),  $\text{V}_2\text{O}_5$ ,  $\text{V}_6\text{O}_{13}$ ,  $\text{LiV}_3\text{O}_8$  and  $\text{LiNaV}_2\text{O}_5$  were found to show superior electrochemical properties [8–16]. It is feasible to insert reversibly about 2.2 Li per molybdenum in molybdenum oxides [17]. Molybdenum-containing compounds exhibit a large reversible capacity when employed as negative electrodes [18–23]. Based on all these observations, it is concluded that vanadium- and molybdenum-containing oxides offer better electrochemical activity due to V and Mo in contrast to phosphates and sulphates.

$\text{MoV}_2\text{O}_8$ , brannerite-type  $\text{LiVMoO}_6$  and  $\text{VoMoO}_4$  were recently explored for lithium insertion [24–26].

$\text{AlVMoO}_7$  crystallizes in the orthorhombic system and the structure is composed of corner-shared tetrahedral polyanionic groups. It forms isolated edge-shared  $\text{Al}_2\text{O}_{10}$  octahedral dimers when coordinated to  $\text{Al}^{3+}$  (figure 1). The columns of both edge-shared  $\text{Al}_2\text{O}_{10}$  octahedral dimers and corner-shared  $(\text{Mo/V})_2\text{O}_7$  tetrahedral clusters run parallel to the *c*-axis. These columns share the corners to form a three-dimensional network. One oxygen per formula unit [O (1)] is bonded to one Mo/V atom forming  $(\text{Mo/V})=\text{O}$  oxo-linkage [27].

The present work investigates electrochemical insertion of lithium on a sol–gel synthesized  $\text{AlVMoO}_7$  sample. The redox couples of V/Mo and the cavities present in the structure were investigated to determine the facile insertion/extraction of Li in  $\text{AlVMoO}_7$ .

## 2. Experimental

### 2.1 Synthesis

**2.1a Sol–gel synthesis (SG):** In SG synthesis method,  $\text{MoO}_3$  powder (Cerac, 99.9%) was dissolved in a mixture of 40 ml of 30%  $\text{H}_2\text{O}_2$  and 10 ml of  $\text{NH}_4\text{OH}$ , resulting in a clear solution (A). Since the reaction is exothermic; it was carried out in an ice bath.  $\text{NH}_4\text{VO}_3$  was dissolved in hot water and subsequently,  $\text{Al}(\text{NO}_3)_3$  was added to this solution (B). A solution of citric acid at 3:1 molar ratio was added to a mixture of solutions A and B under constant stirring; this led to the formation of a sol and then ethylene glycol was added to this for gel formation. After stirring for 5 h, a transparent gel was obtained. The gel was decomposed by heating at 90°C

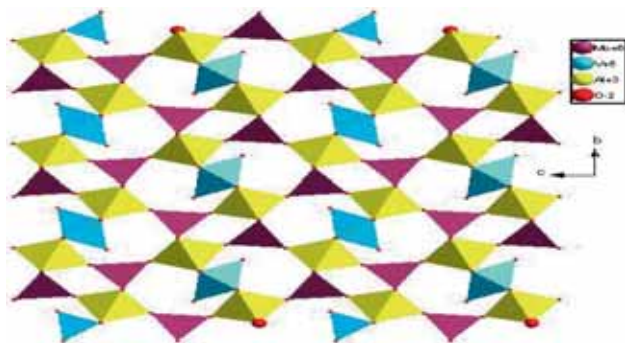


**Figure 1.** Crystal structure of AIVMoO<sub>7</sub> along bc-plane [27].

for 12 h. The final heat treatment for the compound AIVMoO<sub>7</sub> was 550°C for 12 h.

## 2.2 Characterization

Powder X-ray diffraction patterns (PXRD) were analysed using a Rigaku MiniFlex X-ray diffractometer with CuK<sub>α</sub> radiation. The morphology of the sample was analysed using scanning electron microscope (SEM, FEI Quanta 200). Galvanostatic charge/discharge cycling was determined using an Arbin battery cycling unit (Arbin Instruments, BT 2000, USA). *Ex situ* XRD characterization was carried out by using Rigaku miniflex X-ray diffractometer in the 2θ range of 10°–70°.

The Swagelok cells (Swagelok India, Bangalore) were dismantled in the glove box. In addition to this, the electrodes were covered with a Mylar film and the obtained XRD patterns were used for the *ex situ* XRD studies. Swagelok cells were used to analyse electrochemical lithium insertion/extraction. The electrodes were fabricated by dispersing a blend of 70 wt% active material, 20 wt% acetylene black (Denka Singapore Pvt. Ltd.) with 10 wt% PVDF in N-methyl-2-pyrrolidinone on a stainless steel foil (as a disc of 14 mm diameter) and dried in an oven at 100°C for 12 h. An argon-filled glove box (mBraun, 120G, Germany) was used to assemble the Swagelok cells. Lithium metal (Aldrich, 99.9%) was used as the counter electrode and Teklon (Anatek, USA) as the separator. All the tests were performed using 1 M LiPF<sub>6</sub> dissolved in the mixture of 1:1 ethylene carbonate + dimethyl carbonate (Chile Industries Ltd., Korea) as the electrolyte. For the electrochemical experiments, the cells were equilibrated for 12 h at room temperature. *Ex situ* XRD description of the electrodes was processed in the 2θ range of 10°–70° by covering the electrodes with a Mylar film.

## 3. Results and discussion

### 3.1 Phase formation

The PXRD pattern of AIVMoO<sub>7</sub> is shown in figure 2. The pattern is indexed based on JCPDS file no. 89–0871 for

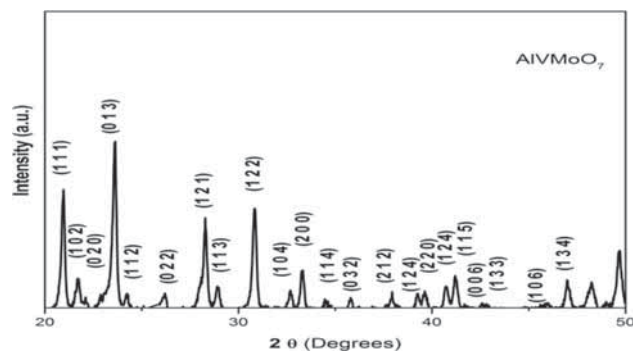


**Figure 2.** PXRD pattern of AIVMoO<sub>7</sub>.

**Table 1.** Cell parameters for the three samples: AIVMoO<sub>7</sub>, Li<sub>0.5</sub>AIVMoO<sub>7</sub> and Na<sub>0.5</sub>AIVMoO<sub>7</sub>.

Lattice parameters	AIVMoO <sub>7</sub>	Li <sub>0.5</sub> AIVMoO <sub>7</sub>	Na <sub>0.5</sub> AIVMoO <sub>7</sub>
<i>a</i> (Å)	5.3760(0)	5.3600	5.3760(0)
<i>b</i> (Å)	8.1600(1)	8.1580	8.1580(1)
<i>c</i> (Å)	12.7211(3)	12.7100	12.7100(3)
<i>α</i> (°)	90.000(1)	90.000(1)	90.000
<i>β</i> (°)	90.000	90.000	90.000(1)
<i>γ</i> (°)	90.000(2)	90.000(2)	90.000
Cell volume (Å <sup>3</sup> )	558.1(2)	558.8(2)	555.6

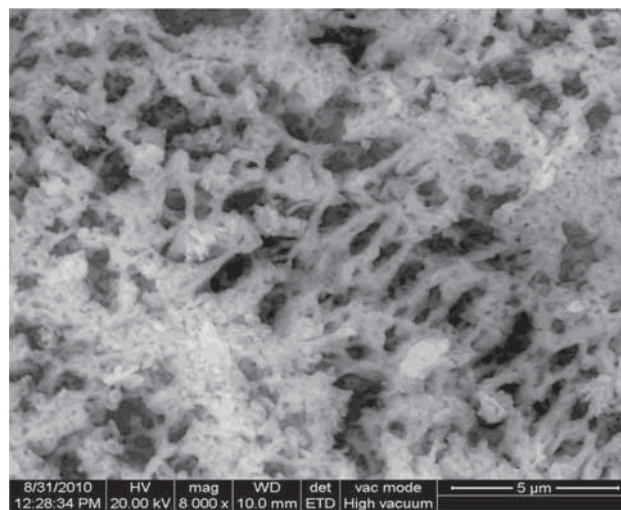


**Figure 3.** SEM micrograph of AIVMoO<sub>7</sub>.

AIVMoO<sub>7</sub> and confirms that only a single phase is formed. The calculated lattice parameters are in agreement with those reported in earlier studies (table 1) [27]. Figure 3 presents SEM image of AIVMoO<sub>7</sub>. The microstructure collaborates well with the final calcination temperature/time. The calcination temperature and time for AIVMoO<sub>7</sub> were significantly lower, thus, very porous structure was formed.

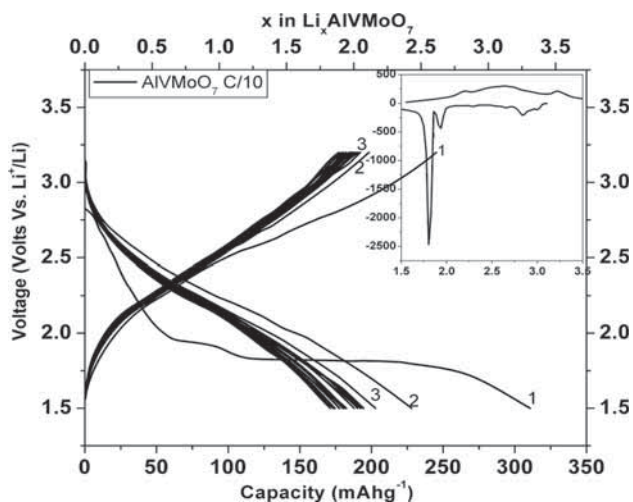


**Figure 4.** Electrochemical charge–discharge curves of  $\text{AIVMoO}_7$ . The inset shows the corresponding differential capacity plot ( $dQ/dV$ ).

### 3.2 Electrochemical studies

**3.2a  $\text{AIVMoO}_7$ :** The voltage–capacity–composition profile of  $\text{AIVMoO}_7$  vs.  $\text{Li}^+/\text{Li}$  cell and the corresponding differential capacity plot are shown in figure 4. The charge–discharge curves were obtained galvanostatically at  $C/10$  rate (reaction of one Li in 10 h). During initial discharge, a drop in the voltage of the cell from the open circuit voltage of 3.1–3.07 V was noted. During the first discharge, the system showed the capacity of  $310 \text{ mAh g}^{-1}$ . This corresponds to the reaction of 3.3 Li per formula unit. The first charge capacity was found to be  $245 \text{ mAh g}^{-1}$  corresponding to the extraction of 2.6 Li. Three plateaus were observed at 2.8, 1.9 and 1.8 V in the differential capacity plot. However, the assignments of the plateaus will differ, if the phases contain both V and Mo in the same lattice. In  $\text{MoV}_2\text{O}_8$ , the major reduction progression was noted at 2.5–2 V, which could be attributed to both redox couples  $\text{V}^{5+}/\text{V}^{4+}$  and  $\text{Mo}^{6+}/\text{Mo}^{5+}$  [24] and in the case of  $\text{LiVMoO}_6$ , a single plateau at 2.4 V was observed attributable to the reduction of  $\text{Mo}^{6+} \rightarrow \text{Mo}^{5+}$  and  $\text{V}^{5+} \rightarrow \text{V}^{4+}$  [25]. Two clearly discernible plateaus were observed at about 2.1 and 1.7 V, which were attributed to  $\text{Mo}^{6+}/\text{Mo}^{5+}$ ,  $\text{Mo}^{5+}/\text{Mo}^{4+}$  reduction in the case of  $\text{Ni}_2(\text{MoO}_4)_3$  [28]. Thus, considering the literature reports, it can be concluded that the plateaus at 2.8 and 1.9 V can be attributed to the reduction of  $\text{V}^{5+} \rightarrow \text{V}^{4+}$  and  $\text{Mo}^{6+} \rightarrow \text{Mo}^{5+}$ , respectively [24,25,28]. In addition, the plateau at 1.8 V can be attributed to the reduction of  $\text{Mo}^{5+}/\text{Mo}^{4+}$  [28]. Out of the 3.3 Li reacted during the first discharge in  $\text{AIVMoO}_7$ , the reaction of two Li can be attributed to the reduction of  $\text{V}^{5+} \rightarrow \text{V}^{4+}$  and  $\text{Mo}^{6+} \rightarrow \text{Mo}^{5+}$  and one Li can be ascribed to the reduction of  $\text{Mo}^{5+}/\text{Mo}^{4+}$  in the redox couple. The remaining 0.3 Li reacted was involved in the further partial reduction of V and Mo [24,25,28].

The PXRD patterns recorded on the parent electrode, as well as the electrodes discharged up to different cut-off

voltages, are shown in figure 5. The intensity of the main peaks progressively decreased with the lithiation and fully disappeared after the discharge. After charging the electrodes, the Bragg peaks completely vanished in the PXRD patterns. An irreversible phase transformation into amorphous lithiated phases occurred during the first discharge. The occurrence of amorphization during the first discharge was reported for various vanadates and molybdates in several studies [29–32].

In  $\text{AIVMoO}_7$  phase,  $\text{Mo}^{6+}$  and  $\text{V}^{5+}$  were found to exist in the tetrahedral coordination, whereas the reduced species in the lithiated phase, viz.  $\text{Mo}^{5+}$  and  $\text{V}^{4+}$ , appeared not favouring the tetrahedral coordination. They were found generally not accepting tetrahedral geometry as both  $\text{Mo}^{4+}$  or  $\text{Mo}^{5+}$  and  $\text{V}^{4+}$  were bigger in size. This indicates the loss of structural integrity as a function of lithium reaction, which leads to the observed fading of the capacity [28].

*Ex situ* PXRD patterns were recorded for the electrodes at various stages of lithium reaction to monitor the structural changes (figure 6). The reaction of 1.0 Li did result in any major changes in the PXRD pattern. However, upon reaction of 3 Li, an apparent change was seen in the PXRD pattern. The phase remained ‘X-ray amorphous’, even after a charge cycle [29–32].

The solid solution regime was more prevalent in the case of  $\text{AIVMoO}_7$  (0.5 Li). We believe that 0.5 Li is inserted and the remaining is reacted in the case of  $\text{AIVMoO}_7$ . To prove that the insertion is feasible in this lattice, the chemical insertion of sodium into  $\text{AIVMoO}_7$  phase was carried out using the reducing agent sodium azide ( $\text{NaN}_3$ ). This alkali metal azide can decompose easily at elevated temperature to the alkali metal and nitrogen, and acts as an intercalating agent. The sodium intercalated phase,  $\text{Na}_{0.5}\text{AIVMoO}_7$ , was prepared by heating the stoichiometric amounts of  $\text{NaN}_3$  and  $\text{AIVMoO}_7$  in an evacuated and sealed quartz tube at  $350^\circ\text{C}$  for 6 h (in pellet form). The intercalated phase of  $\text{Na}_{0.5}\text{AIVMoO}_7$  was characterized by PXRD, which showed a single phase, where all the reflections could be indexed on the basis of the orthorhombic unit cell with space group  $P\ mcn$  (62). The analysis of the PXRD patterns of  $\text{Na}_{0.5}\text{AIVMoO}_7$  and  $\text{Li}_{0.5}\text{AIVMoO}_7$  indicated that the orthorhombic structure of the parent  $\text{AIVMoO}_7$  phase is retained and the lattice parameters are decreased slightly. The calculated lattice parameters are given in table 1 [27]. The chemical insertion experiment demonstrated that the structure is stable with the insertion of alkali in the extent of 0.5 per formula unit corroborating well with the solid solution behaviour observed from the voltage–capacity–composition curves. A constant specific capacity of  $180 \text{ mAh g}^{-1}$  was observed in  $\text{AIVMoO}_7$  even after 20 cycles.

## 4. Conclusion

In this study, we determined the effects of electrochemical insertion of Li in  $\text{AIVMoO}_7$ . It was observed that the voltage corresponding to the redox couples  $\text{V}^{5+}/\text{V}^{4+}$  and  $\text{Mo}^{6+}/\text{Mo}^{5+}$  were significantly different for  $\text{AIVMoO}_7$ . It can

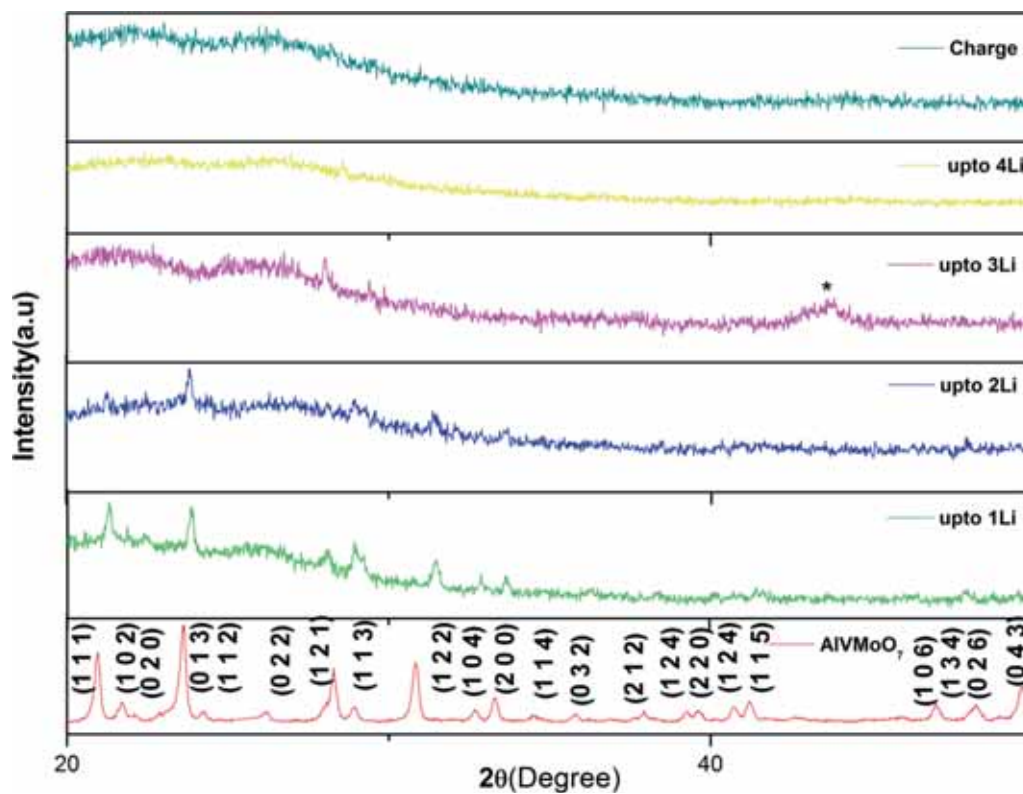


**Figure 5.** *Ex situ* XRD patterns of  $\text{AlVMoO}_7$ : (a) before discharge, up to (b) 1 Li, (c) 2 Li, (d) 3 Li, (e) after the first discharge and (f) after the first cycle.

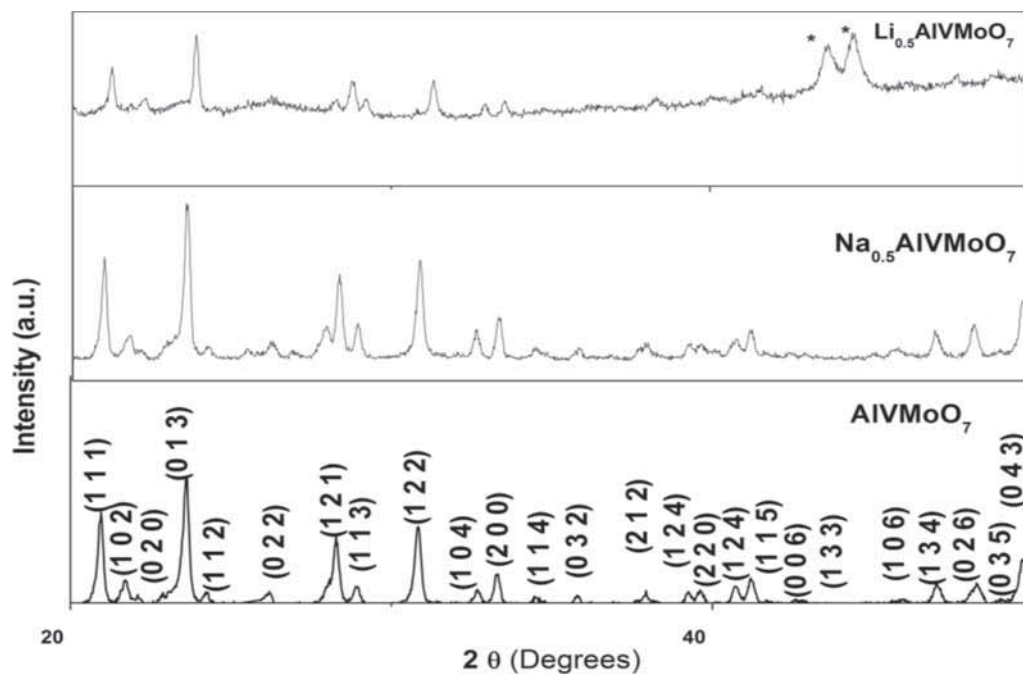


**Figure 6.** PXRD patterns of  $\text{AlVMoO}_7$ : after (a) 0.5 Na and (b) 0.5 Li.

be affirmed that sodium insertion is also possible in the lattice up to 0.5 Na.  $\text{AlVMoO}_7$  can accommodate 3.3 Li per formula unit, of which the reaction of 2.6 Li only is reversible. The results of cycling studies showed that the  $\text{AlVMoO}_7$  phase exhibits a reversible capacity of 180 mAh  $\text{g}^{-1}$  without any noticeable fading even after 20 cycles. The reversibility of Li reaction was more facile in  $\text{AlVMoO}_7$ .

### Acknowledgements

This work was carried out in Indian Institute of Technology, IIT, Madras and IITM is gratefully acknowledged. It is my immense pleasure to express my sincere thanks and deep sense of gratitude to my research supervisor Prof U V Varadaraju for his useful suggestions rendered during my research.

### References

- [1] Shirakawa J, Nakayama M, Wakihara M and Uchimoto 2007 *J. Phys. Chem. B* **111** 1424
- [2] Alvarez-Vega M, Amador U, Arroyo-De M E and Dompablo M 2005 *J. Electrochem. Soc.* **152** A1306
- [3] Leyzerovich N N, Bramnik K G, Buhmester T, Ehrenberg H and Fuess 2004 *J. Power Sources* **127** 76
- [4] Morcrette M, Rozier P, Dupont L, Mugnier E, Sannier L, Galy J *et al* 2003 *Nat. Mater.* **2** 755
- [5] Morcrette M, Martin P, Rozier P, Vezin H, Chevallier F, Laffont L *et al* 2005 *Chem. Mater.* **17** 418
- [6] Begam K M, Michael M S, Yap Y H T and Prabaharan S R S 2004 *Electrochem. Solid-State Lett.* **7** A242
- [7] Prabaharan S R S, Michael M S and Begam K M 2004 *Electrochem. Solid-State Lett.* **7** A416
- [8] Zachau-Christiansen B, West K and Jacobsen T 1985 *Mater. Res. Bull.* **20** 485
- [9] Murphy D W, Christian P A, Disalvo F J and Waszczak J V 1979 *Inorg. Chem.* **18** 2800
- [10] Murphy D W, Christian P A, Disalvo F J, Carides J N and Waszczak J V 1981 *Electrochem. Soc.* **128** 2053
- [11] Pistoia G, Pasquali M, Wang G and Li L 1990 *J. Electrochem. Soc.* **137** 2365
- [12] Bouhedja L, Castro-Garcia S, Livage J and Julien C 1998 *Ionics* **4** 227
- [13] Denis S, Baudrin E, Touboul M and Tarascon J M 1997 *J. Electrochem. Soc.* **144** 4099
- [14] Takeda Y, Itoh K, Kanno R, Icikawa T, Imamshi N and Yamamoto O 1991 *J. Electrochem. Soc.* **138** 2566
- [15] Andrukaitis E 1995 *J. Power Sources* **54** 470
- [16] Patoux S and Richardson T J 2007 *Electrochem. Commun.* **9** 485
- [17] Song J, Wang X, Ni X, Zheng H, Zhang Z, Ji M *et al* 2005 *Mater. Res. Bull.* **40** 1751
- [18] Leroux F and Nazar L 2000 *Solid State Ionics* **133** 37
- [19] Tsumura T and Inagaki M 1997 *Solid State Ionics* **104** 183
- [20] James A C W P and Goodenough J B 1988 *J. Solid State Chem.* **76** 87
- [21] Huang C-K, Crouch-Baker S and Huggins R A 1988 *J. Electrochem. Soc.* **135** 408
- [22] Begam K M and Prabaharan S R S 2006 *J. Power Sources* **159** 319
- [23] Michael M S, Begam K M, Michael Cloke and Prabaharan S R S 2008 *J. Solid State Electrochem.* **12** 1025
- [24] West K, Zachau-Christiansen B, Skaarup S and Jacobson T 1992 *Solid State Ionics* **53** 356
- [25] Tranchant A and Messina R 1988 *J. Power Sources* **24** 85
- [26] Amdouni N, Zarrouk H, Soulette F and Julien C M 2003 *J. Mater. Chem.* **13** 2374
- [27] Anji Reddy M, Satya Kishore M, Pralong V, Caignaert V, Varadaraju U V and Raveau B 2007 *J. Power Sources* **168** 509
- [28] Prabaharan S R S, Michael M S, Ramesh S and Begam K M 2004 *J. Electroanal. Chem.* **570** 107
- [29] Guyomard D, Sigala C, Salle A G L and Piffard Y 1997 *J. Power Sources* **68** 692
- [30] Rossignol C, Ouvrad G and Baudrin E 2001 *J. Electrochem. Soc.* **148** A869
- [31] Kim S, Ogura S, Ikuta H, Uchimoto Y and Wakihara M 2002 *Solid State Ionics* **146** 249
- [32] Laruelle S, Poizot P, Baudrin E, Briois V, Touboul M and Tarascon J M 2001 *J. Power Sources* **97–98** 251